HHS Public Access

Author manuscript

Cell Calcium. Author manuscript; available in PMC 2023 May 01.

Published in final edited form as:

Cell Calcium. 2022 May ; 103: 102564. doi:10.1016/j.ceca.2022.102564.

Dynamin 1 controls vesicle size and endocytosis at hippocampal synapses

Bo Shi[1,2,*], **Ying-Hui Jin**[1,3,*], **Ling-Gang Wu**[1,◆]

[1]National Institute of Neurological Disorders and Stroke, 35 Convent Dr., Bethesda, MD 20892

[2]Biological Sciences Graduate Program, College of Computer, Mathematical, and Natural Sciences, University of Maryland, College Park, MD 20740

[3]Current address: Department of Critical Care Medicine, Nanfang Hospital, Southern Medical University, 1838 North Guangzhou Ave, Guangzhou, China 510515

Abstract

Following calcium-triggered vesicle exocytosis, endocytosis regenerates vesicles to maintain exocytosis and thus synaptic transmission, which underlies neuronal circuit activities. Although most molecules involved in endocytosis have been identified, it remains rather poorly understood how endocytic machinery regulates vesicle size. Vesicle size, together with the transmitter concentration inside the vesicle, determines the amount of transmitter the vesicle can release, the quantal size, that may control the strength of synaptic transmission. Here, we report that, surprisingly, knockout of the GTPase dynamin 1, the most abundant brain dynamin isoform known to catalyze fission of the membrane pit's neck (the last step of endocytosis), not only significantly slowed endocytosis but also increased the synaptic vesicle diameter by as much as ~40–64% at cultured hippocampal synapses. Furthermore, dynamin 1 knockout increased the size of membrane pits, the precursor for endocytic vesicle formation. These results suggest an important function of dynamin other than its well-known fission function – control of vesicle size at the pit formation stage.

Graphical Abstract

◆:Corresponding author, wul@ninds.nih.gov.
*:Equal contribution

Declaration of interest

The authors declare no competing financial interests.

CRediT author statement

Bo Shi: Methodology, Investigation, Data Curation, writing – Original Draft, Visualization. **Ying-Hui Jin:** Methodology, Investigation, Data Curation. ***Ling-Gang Wu***: Supervision, writing – Review & Editing, Visualization.

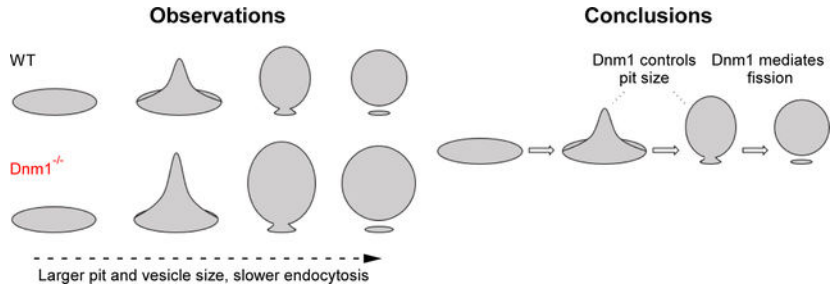

Keywords

dynamin; endocytosis; vesicle size; vesicle recycling; synaptic transmission; hippocampus

1. Introduction

Calcium influx triggers vesicle fusion, fusion pore opening, and release of vesicular lumen transmitters and hormones, which mediate synaptic transmission and control animal behaviors [1]. Opening of the vesicular fusion pore at the plasma membrane generates an Ω-shape membrane profile, which may close its pore (termed kiss-and-run or close fusion) or merge with the plasma membrane by shrinking of the Ω-profile or by dilating its pore until flattening of the Ω-profile [2–12]. Merging of the Ω-profile with the plasma membrane is followed by classical endocytosis, which transforms flat plasma membrane into oval/round vesicles [2, 13]. Classical endocytosis, together with kiss-and-run, recycles vesicles and thus sustains synaptic transmission [1, 14–16]. Over the last several decades many proteins and lipids involved in classical endocytic curvature transition have been identified. The most ubiquitous protein involved in nearly all forms of endocytosis and kiss-and-run is dynamin, a GTPase that catalyzes fission pore or fusion pore closure [9, 11, 17–20, but see Refs. 21, 22]. Despite these significant advancements, our understanding of the mechanisms that control endocytic vesicle size remains rather poor. Vesicle size is important for nerve terminals to maintain calcium-triggered exocytosis, which mediates the synaptic transmission crucial for neuronal circuit function. It is the vesicle size, together with the vesicular transmitter concentration, that determines the quantal size, a basic parameter that determines synaptic strength [23–27]. If vesicles were much bigger than normal, a nerve terminal would contain much fewer vesicles that can be exhausted much more rapidly during high-frequency firing, resulting in much faster depression or even failure of synaptic transmission. Furthermore, bigger vesicles may generate larger quantal size [23–27], making it more difficult to fine tune transmitter release. For cell types not involved in secretion, vesicle size is important in determining what endocytosis can take up, such as large viruses, toxins, solutions, or membrane-associated proteins. It may also determine the efficiency and dynamics of endocytosis for a given cell to use either small but frequent vesicle uptake or large but infrequent vesicle making [1].

Deletion of clathrin adaptor protein 180 (AP180) increases the vesicle size by about ~20% and the quantal size by ~60%, suggesting that AP180 is involved in controlling vesicle size [25]. The involvement of AP180 in controlling vesicle size seems to imply the involvement

of clathrin in controlling vesicle size. However, perturbation of clathrin did not always affect vesicle size. Acute photoinactivation of clathrin light chain or clathrin heavy chain blocks vesicle generation, causes accumulation of large internal membrane compartments, and increases vesicle size at *Drosophila* neuromuscular junctions [28, 29]. In contrast, mutation of clathrin heavy chain in *C. elegans*, which impairs receptor-mediated endocytosis, reduces synaptic vesicle size by ~14% [30]. Knockdown of clathrin did not significantly affect ultrafast endocytosis or slow endocytosis at mouse hippocampal synapses [31, 32, but see Ref. 33], but did not cause a significant change in synaptic vesicle sizes [31, 32]. In summary, understanding of the endocytic molecules involved in regulation of vesicle size is poor relative to understanding of general molecular mechanisms of endocytosis.

In the present work, we found that knockout of dynamin 1, the main dynamin isoform in the brain [34], increased the vesicle diameter by as much as ~40% at hippocampal nerve terminals. This is a surprising finding, because dynamin has been well known for several decades as a GTPase mediating cutting of the membrane pit's neck, resulting in formation of an endocytic vesicle. This finding suggests that dynamin 1 has an additional crucial function in endocytosis – controlling vesicle size at central synapses. Furthermore, dynamin 1 plays a more critical role than previously recognized at central synapses, because dynamin 1 knockout at hippocampal synapses generated a much larger block of endocytosis measured after low and high-frequency action potential trains than previously reported at cortical synapses [34, 35].

2. Results

2.1. Dynamin 1 knockout severely inhibits endocytosis after 5–40 Hz action potential trains

Dynamin 1 knockout slows down endocytosis significantly only *during* high-frequency firing, but not *after* high or low frequency firing, at conventional small boutons of cortical synapses [34, 35]. To determine whether this observation applies beyond cortical synapses, endocytosis was examined at hippocampal synapses lacking dynamin 1. To detect endocytosis, the hippocampal cultures were transfected with pH-sensitive synaptophysin-pHluorin2X (SypH). Application of a 10 s train of stimuli (1 ms/20 mA) at 20 Hz ($Train_{20Hz}$), which generates an action potential train [36, 37], induced a SypH fluorescence (F_{SypH}) increase (ΔF) and then decrease, reflecting exocytosis and then endocytosis, respectively (Fig. 1A, B) [38].

In wild-type (WT) control culture at 22–24°C, the initial F_{SypH} decay rate ($Rate_{decay}$) was 5.5 ± 0.5%/s, which was calculated after normalizing the ΔF to 100%. ΔF/F was 316 ± 52% over the baseline fluorescence intensity F (n = 11 experiments, 1–3 experiments per culture, 6 cultures, each culture from 3–6 mice; Fig. 1C). In dynamin $1^{-/-}$ ($Dnm1^{-/-}$) cultures, dynamin 1 was knocked out, as verified with western blot (Fig. S1) [34]; F_{SypH} decay was much slower as compared to control (Fig. 1A, B), the $Rate_{decay}$ was significantly reduced to ~41% of the WT level (Fig. 1C), and ΔF/F was also reduced substantially (Fig. 1A, C). While these results were obtained at room temperature, similar results were obtained at physiological temperature (34–37°C) after action potential trains at 20 Hz (WT, 6 experiments; $Dnm1^{-/-}$, 4 experiments) and 40 Hz (WT, 5 experiments; $Dnm1^{-/-}$,

4 experiments; Fig. S2). The slower F_{SypH} decay time course, smaller $Rate_{decay}$, and smaller ΔF found in $Dnm1^{-/-}$ cultures were rescued to the control level by transfecting WT dynamin 1 (Dnm1) to these cultures (Fig. 1A–C).

To exclude the possibility that the slower F_{SypH} decay in $Dnm1^{-/-}$ culture is not due to slower reacidification, MES solution with a pH of 5.5 was applied before and after the $Train_{20Hz}$. Before $Train_{20Hz}$, the MES solution quenched F_{SypH} to the background level, resulting in a decrease of F_{SypH} by ΔS (Fig. 1D), which reflected the preexisting SypH molecules at the plasma membrane surface. Washing out the MES solution led to recovery of F_{SypH} to baseline (Fig. 1D). Then, $Train_{20Hz}$ was applied to induce exo-endocytosis (Fig. 1D). At 10 s after $Train_{20Hz}$, when F_{SypH} remained well above baseline, MES solution was applied again, which quenched F_{SypH} to a level similar to that during MES application before $Train_{20Hz}$ (lower dash line; Fig. 1D), but much lower than that predicted (F_{sypH} decrease by ΔS) if F_{SypH} decay were due to reacidification (upper dash line; Fig. 1D, n = 5). F_{SypH} recovered above baseline after MES washout, confirming the prolonged presence of SypH at the plasma membrane (Fig. 1D). Thus, slower F_{SypH} decay in $Dnm1^{-/-}$ cultures primarily reflected slower endocytosis.

The slower F_{SypH} decay was accompanied by a reduction of ΔF, suggesting that exocytosis is reduced. However, reduction of ΔF is not the reason for the slower F_{SypH} decay, because smaller ΔF induced by a 2 s train of stimulation at 20 Hz or by a lower frequency stimulation train does not prolong F_{SypH} decay [37, 39] (see also Fig. 2, 5-Hz train). Rather, inhibition of endocytosis may account for the reduction of ΔF, because endocytosis may facilitate vesicle replenishment to the readily releasable pool during repetitive stimulation by facilitation of active zone clearance after exocytosis [1, 40, 41]. Consistent with this explanation, inhibition of proteins involved in endocytosis, such as dynamin, calcineurin, calmodulin, actin, and potassium channel Kv3.3 has been shown to slow down endocytosis and reduce exocytosis during repetitive stimulation [37, 39, 40, 42, 43].

Next, we determined whether the slower F_{SypH} decay in $Dnm1^{-/-}$ cultures depended on the frequency of stimulation. F_{SypH} decay was slower with a smaller $Rate_{decay}$ after a 10 s action potential train at 40 Hz (Fig. 2A–C) and at 5 Hz (Fig. 2D–F) in $Dnm1^{-/-}$ cultures. $Rate_{decay}$ in $Dnm1^{-/-}$ cultures was 65 ± 12% (n = 8) of that in WT control after the 5-Hz train, but 41 ± 2% (n = 6) and 33 ± 8% (n = 6) of that in WT control after the 20-Hz and 40-Hz train, respectively (Fig. 2G). The $Rate_{decay}$ reduction after the 5-Hz train was not as significant as those after 20-Hz or 40-Hz train (Fig. 2G). Thus, dynamin 1 is important in mediating endocytosis after both low and high-frequency firing, but more crucial after higher frequency firing.

2.2. Dynamin 1 knockout enlarges membrane pits and thus their resulting vesicles

In WT hippocampal cultures, the vesicle diameter, examined with electron microscopy (EM), ranged from 17 to 249 nm with a mean of 38.6 ± 0.2 nm (n = 2170 vesicles, 22 boutons, 4 cultures, Fig. 3A–C). Among these vesicles, 98.9% (2146 out of 2170 vesicles) had a diameter < 80 nm; their mean diameter was 37.6 ± 0.1 nm (n = 2146 vesicles, Fig. 3D), which reflects the mean diameter of synaptic vesicles. As in previous studies [39, 44], 80 nm was used as the boundary to decide whether vesicles are synaptic vesicles (< 80 nm)

or endosome-like structures (>80 nm). The remaining 1.1% of vesicles had a diameter > 80 nm, which is often called endosome-like structures because their sizes are similar to those of endosomes [39, 44]. These WT control results were similar to previous reports [39, 44].

In Dnm1$^{-/-}$ culture, the vesicle diameter ranged from 22 to 315 nm with a mean of 63.2 ± 0.5 nm (n = 2628 vesicles, 49 boutons, 5 cultures), which was on average ~64% larger than that (38.6 ± 0.2 nm) in WT control (Fig. 3A–C). 80% of vesicles (2101 out of 2628) in Dnm1$^{-/-}$ culture had a diameter < 80 nm; their mean diameter was 52.5 ± 0.3 nm (n = 2101 vesicles), which was on average ~40% larger than the corresponding control (37.6 ± 0.1 nm, n = 2146 vesicles, Fig. 3D). The percentage of vesicles with a diameter > 80 nm was 20%, which was much larger than the corresponding WT control (1.1%). In summary, the mean diameter of all vesicles and synaptic vesicles (diameter < 80 nm) in Dnm1$^{-/-}$ culture were on average ~40–64% larger than the corresponding WT control, suggesting that dynamin 1 is crucial in controlling synaptic vesicle size.

To determine whether the increase in vesicle size in Dnm1$^{-/-}$ nerve terminals is due to formation of large pits, membrane pits in boutons were examined before and 0, 3, and 10 min after 90 mM KCl application for 1.5 min. Membrane pits, which may appear as Λ-shape (or dome shape), ⌒-shape, or Ω-shape (Fig. 4A) were defined as having a height >15 nm, a base of 20–120 nm, and a height/base ratio >0.15 (Fig. 4A). Below these criteria, pits were too small or shallow to identify unambiguously. The pit number per bouton (cross section) peaked at 3–10 min after KCl application (Fig. 4B), likely because endocytosis continued for > 10 min after KCl application [39, 44]. In Dnm1$^{-/-}$ boutons, the pit number after KCl application was significantly higher than in control boutons at every time point measured (Fig. 4B), likely because fission was blocked by dynamin 1 knockout, causing pit accumulation [18, 19]. The pit height (from base membrane) was also significantly higher in Dnm1$^{-/-}$ boutons than in control boutons at all time points before or after KCl application (Fig. 4C). These results suggest that in Dnm1$^{-/-}$ boutons, larger pits are generated after depolarization-induced exocytosis (Fig. 4) and eventually form larger vesicles as observed in resting conditions (Fig. 3) at a much slower rate (Figs. 1, 2). Dynamin 1 is thus a crucial molecule controlling vesicle size at hippocampal synapses (Fig. 4D).

3. Discussion

In the present work, we showed that dynamin 1 knockout significantly slowed endocytosis at cultured hippocampal synapses after action potential trains at 5–40 Hz, with more slowing observed at higher frequency (Figs. 1, 2, S1, S2). These results suggest that dynamin 1 plays a more crucial role at conventional central synapses than previously recognized, given that dynamin 1 knockout at conventional small-bouton cortical synapses inhibited endocytosis strongly only during, not after, high-frequency firing [34, 35]. More importantly, dynamin 1 knockout increased the diameter of synaptic vesicles (< 80 nm) by as much as ~40%, and the diameter of all vesicles by as much as ~64% (Fig. 3). Such increases were accompanied by an increased membrane pit size, the precursor to forming larger vesicles (Fig. 4). These results suggest that dynamin 1 is crucial for not only membrane fission as generally thought, but also controlling synaptic vesicle size at hippocampal synapses (Fig. 4D).

In addition to endocytic flat-to-round transformation, large vesicles could in principle be generated by other mechanisms, such as compound vesicle-vesicle fusion in the cytosol [27, 45], sequential compound vesicle fusion at the plasma membrane followed by kiss-and-run [46], and a form of kiss-and-run involving fusion pore opening, enlargement of the fusion-generated Ω-profile, and closure of the fusion pore (termed enlarge close fusion) [12, 47]. However, these other mechanisms are highly unlikely to contribute to the increase in vesicle size observed in Dnm1$^{-/-}$ synapses, because dynamin 1 knockout may block fusion pore closure [9, 11], which in turn may block large vesicle generation from various forms of kiss-and-run mentioned above. Furthermore, to the authors' knowledge, there has been no report of dynamin preventing compound vesicle-vesicle fusion, which could contribute to the vesicle size increase in Dnm1$^{-/-}$ synapses.

Our observation that synaptic vesicle diameter was enlarged by as large as ~40% in Dnm1$^{-/-}$ hippocampal synapses is a surprising finding. Previous studies reported only an ~8–10% increase in vesicle diameter in Dnm1$^{-/-}$ cortical synapses and calyx-type synapses [34, 48]. Even with dynamin 1 and 3 knockout, vesicle diameter increased by only ~14% [35]. While these results may suggest that dynamin regulates vesicle size, these findings of only small increases have led to a general neglect of this potentially important function of dynamin. The large degree of increase (~40%) at Dnm1$^{-/-}$ hippocampal synapses reported here re-establish dynamin as an important regulator of vesicle size. This function must take place before fission, because membrane pits generated after depolarization were much larger in Dnm1$^{-/-}$ synapses than in WT (Fig. 4). Our finding is consistent with studies suggesting that dynamin facilitates clathrin-coated pit maturation before fission [for review, see Ref. 49]. Therefore, there is evidence to suggest modifying dynamin models to include a new function before fission – control of endocytic membrane pit size and thus resulting endocytic vesicle size (Fig. 4D).

One may ask why dynamin 1 knockout did not increase vesicle size at cortical synapses and calyx-type synapses [34, 35, 48] as much as at the hippocampal synapses reported here. The answer is uncertain, but one possibility is that, at the former synapses, dynamin 1 does not play at as important a role in endocytosis as at hippocampal synapses. Consistent with this possibility, dynamin 1 knockout at conventional small-bouton cortical synapses inhibited endocytosis severely only during, not after, high-frequency firing [34, 35]. These studies led to a view that dynamin 1 is essential only when exocytosis is intense, during high-frequency firing that requires a large endocytic capacity to retrieve many exocytosed vesicles. Other dynamin isoforms have overlapping roles with dynamin 1 and may exercise their roles in the absence of dynamin 1 in mild stimulation conditions. The present work shows that knockout of dynamin 1 alone is sufficient to inhibit endocytosis after low- and high-frequency firing (Figs. 1, 2), suggesting that the role of dynamin 1 in endocytosis after repetitive low- and high-frequency firing at hippocampal synapses is much larger than that at cortical synapses. Consistent with this suggestion, dynamin 1 knockout at the large calyx-type synapse also inhibits endocytosis after prolonged depolarizing pulses [48]. The novel role of dynamin in controlling vesicle size may have wide implications, because many synapses, such as frog or torpedo neuromuscular junctions and calyx of Held synapses, may generate vesicles of various sizes, especially large vesicles, after intense nerve firing [23, 27, 50].

4. Conclusion

The present work shows a much more important role than previously recognized for dynamin 1 in mediating endocytosis, particularly after high-frequency firing at mammalian central synapses. Surprisingly, these results reveal that dynamin 1 is a crucial molecule controlling vesicle size at a step before fission, during formation of membrane pits, at hippocampal synapses. This finding raises the question of how dynamin 1 regulates the size of membrane pits, which seems obviously unrelated to its well-known crucial role in fission. Addressing this question would be a fascinating research topic in the future.

5. Methods

5.1. Animals

Animal care and use were carried out according to NIH guidelines and approved by the NIH Animal Care and Use Committee. Dynamin $1^{+/-}$ ($Dnm1^{+/-}$) mice were purchased from the Jackson Laboratory. $Dnm1^{-/-}$ mice of either sex were obtained by heterozygous breeding using standard mouse husbandry procedures. Mouse genotypes were determined by PCR and verified in some experiments with western blot. Wild-type littermates and wild-type non-littermates of either sex were used as control.

5.2. Hippocampal culture

Mouse hippocampal culture was prepared as described previously [37, 51]. Hippocampal CA1-CA3 regions from P0 mice were dissected, dissociated, and plated on Poly-D-lysine treated coverslips. Cells were maintained at 37°C in a 5% CO_2 humidified incubator with a culture medium consisting of Neurobasal A (Invitrogen, Carlsbad, CA), 10% fetal bovine serum (Invitrogen, Carlsbad, CA), 2% B-27 (Invitrogen, Carlsbad, CA), 0.25% glutamax-1 (Invitrogen, Carlsbad, CA), and 0.25% insulin (Sigma, St. Louis, MO). 5–7 days after plating, neurons were transfected with plasmids using Lipofectamine LTX (Invitrogen, Carlsbad, CA).

Hippocampal cultures were transfected with a plasmid containing synaptophysin tagged with the pH-sensitive pHluorin2X (SypH, provided by Dr. Yong-Ling Zhu) [52] for imaging of endocytosis. cDNA encoding wild-type human Dnm1 was amplified from Dnm1-pmCherryN1 (Addgene #27697). Dnm1 plasmid was transfected along with SypH, and it contained mCherry, which was used to recognize the transfected cells. After transfection, neurons were maintained at 37°C in a 5% CO_2 humidified incubator for another 6–8 days before experiments.

Single action potentials were evoked by a 1 ms pulse (20 mA) through a platinum electrode. The bath solution contained (in mM): 119 NaCl, 2.5 KCl, 2 $CaCl_2$, 2 $MgCl_2$, 25 HEPES (buffered to pH 7.4), 30 glucose, 0.01 6-cyano-7-nitroquinoxaline-2, 3-dione, and 0.05 D,L-2-amino-5-phosphonovaleric acid. The culture chamber for imaging was heated using a temperature controller (TC344B, Warner Instruments, Hamden, CT), which set the temperature during imaging to 34–37°C. Imaging was performed after the culture was at 34–37°C for 15–30 min. The temperature was verified with another small thermometer (BAT-7001H, Physitemp Instruments, Clifton, NJ) in the chamber. SypH images were

acquired at 10 Hz using a Nikon A1 confocal microscope (60X, 1.4 NA), and analyzed with Nikon software.

5.3. Western blot

For Western blot, neurons were washed three times with ice-cold PBS. Cell lysates were prepared in the modified RIPA buffer containing protease inhibitors (Thermo Scientific, Rockford, IL). Equal amounts of proteins, determined by BCA protein assay (Thermo Scientific, Rockford, IL), were loaded onto SDS-PAGE gel and immunoblotted using antibodies against clathrin heavy chain (1:1,000; BD Bioscience, San Jose, CA), dynamin (1:1,000; BD Bioscience, San Jose, CA, recognizing all dynamin isoforms, including 1, 2 and 3), dynamin 1 (1:1,000; Thermofisher, Waltham, MA) and β-actin (1:2,000; Abcam, Cambridge, United Kingdom).

5.4. Electron microscopy

Hippocampal cultures were fixed with 4% glutaraldehyde (freshly prepared, Electron microscopy sciences, Hatfield, PA) in 0.1 N Na-cacodylate buffer solution for at least one hour at 22–24°C, and stored in a 4°C refrigerator overnight. The next day, cultures were washed with 0.1 N cacodylate buffer, treated with 1% OsO_4 in cacodylate buffer for 1 hr on ice, treated with 0.25% uranyl acetate in acetate buffer at pH 5.0 overnight at 4°C, dehydrated with ethanol, and embedded in epoxy resin. Thin sections were counterstained with uranyl acetate and lead citrate, then examined in a JEOL 200 CX TEM. Images were collected with a CCD digital camera system (XR-100 from AMT, Danvers, MA) at a primary magnification of 10,000–20,000X. Synapses were selected based on the structural specialization including synaptic vesicle clustering, synaptic cleft and the postsynaptic density.

5.5. Data collection and measurements of the decay time constant and $Rate_{decay}$

The F_{SypH} increase after stimulation was followed by exponential decay. Instead of measuring the time constant of the decay, we measured the initial rate of the decay in the first 4–10 s after stimulation [37, 39, 43, 53, 54]. The reason we did not measure the decay time constant was that many manipulations, including dynamin 1 knockout in the present work, blocked F_{SypH} decay, making it difficult to reliably quantify the decay time constant within our recording time [37, 39, 43, 53, 54].

5.6. Experimental Design and Statistical Analyses

Means were presented as ± s.e.m. The statistical test was t-test. We used t-test with equal variance, although t-test with unequal variance gave the same result. For pHluorin imaging, each experiment included 20–30 boutons showing fluorescence increase (region of interest: 2 μm × 2 μm). ~1–3 experiments were taken from 1 culture. Each culture was from 3–5 mice. Each group of data was obtained from at least three batches of cultures (3–7 cultures).

Supplementary Material

Refer to Web version on PubMed Central for supplementary material.

Acknowledgements

This work was supported by the National Institute of Neurological Disorders and Stroke Intramural Research Program in USA (ZIA NS003009-15 and ZIA NS003105-10). Bo Shi is in the individual graduate partnership program between the NIH and University of Maryland. Yinghui Jin was in the individual graduate partnership program between the NIH and Southern Medical University, Guangzhou, China. We thank Susan Cheng, Virginia Crocker and Sandra Lara for EM technical support. We thank Nicholas Cordero for English edits to the manuscript.

Abbreviations:

AP180	clathrin adaptor protein 180
Dnm1	dynamin 1
τ	time constant
SypH	synaptophysin-pHluorin2X
F_{SypH}	synaptophysin-pHluorin2X fluorescence
ΔF	synaptophysinp-Hluorin2X fluorescence increase
WT	wild-type
$Rate_{decay}$	the initiate rate of synaptophysin-pHluorin2X fluorescence decay

References

[1]. Wu LG, Hamid E, Shin W, Chiang HC, Exocytosis and endocytosis: modes, functions, and coupling mechanisms, Annu. Rev. Physiol, 76 (2014) 301–331. [PubMed: 24274740]

[2]. Heuser JE, Reese TS, Evidence for recycling of synaptic vesicle membrane during transmitter release at the frog neuromuscular junction, J. Cell Biol, 57 (1973) 315–344. [PubMed: 4348786]

[3]. Ceccarelli B, Hurlbut WP, Mauro A, Turnover of transmitter and synaptic vesicles at the frog neuromuscular junction, J. Cell Biol, 57 (1973) 499–524. [PubMed: 4348791]

[4]. Albillos A, Dernick G, Horstmann H, Almers W, Alvarez de Toledo G, Lindau M, The exocytotic event in chromaffin cells revealed by patch amperometry, Nature, 389 (1997) 509–512. [PubMed: 9333242]

[5]. Klyachko VA, Jackson MB, Capacitance steps and fusion pores of small and large-dense-core vesicles in nerve terminals, Nature, 418 (2002) 89–92. [PubMed: 12097912]

[6]. He L, Wu XS, Mohan R, Wu LG, Two modes of fusion pore opening revealed by cell-attached recordings at a synapse, Nature, 444 (2006) 102–105. [PubMed: 17065984]

[7]. Vardjan N, Stenovec M, Jorgacevski J, Kreft M, Zorec R, Subnanometer fusion pores in spontaneous exocytosis of peptidergic vesicles, J. Neurosci, 27 (2007) 4737–4746. [PubMed: 17460086]

[8]. Zhang Q, Li Y, Tsien RW, The dynamic control of kiss-and-run and vesicular reuse probed with single nanoparticles, Science, 323 (2009) 1448–1453. [PubMed: 19213879]

[9]. Zhao WD, Hamid E, Shin W, Wen PJ, Krystofiak ES, Villarreal SA, Chiang HC, Kachar B, Wu LG, Hemi-fused structure mediates and controls fusion and fission in live cells, Nature, 534 (2016) 548–552. [PubMed: 27309816]

[10]. Jorgacevski J, Kreft M, Zorec R, Exocytotic fusion pores as a target for therapy, Cell Calcium, 66 (2017) 71–77. [PubMed: 28807151]

[11]. Shin W, Ge L, Arpino G, Villarreal SA, Hamid E, Liu H, Zhao WD, Wen PJ, Chiang HC, Wu LG, Visualization of Membrane Pore in Live Cells Reveals a Dynamic-Pore Theory Governing Fusion and Endocytosis, Cell, 173 (2018) 934–945. [PubMed: 29606354]

[12]. Shin W, Arpino G, Thiyagarajan S, Su R, Ge L, McDargh Z, Guo X, Wei L, Shupliakov O, Jin A, O'Shaughnessy B, Wu LG, Vesicle Shrinking and Enlargement Play Opposing Roles in the Release of Exocytotic Contents, Cell Rep, 30 (2020) 421–431 e427. [PubMed: 31940486]

[13]. Shin W, Wei L, Arpino G, Ge L, Guo X, Chan CY, Hamid E, Shupliakov O, Bleck CKE, Wu LG, Preformed Omega-profile closure and kiss-and-run mediate endocytosis and diverse endocytic modes in neuroendocrine chromaffin cells, Neuron, 109 (2021) 3119–3134 e3115. [PubMed: 34411513]

[14]. Saheki Y, De Camilli P, Synaptic vesicle endocytosis, Cold Spring Harb. Perspect. Biol, 4 (2012) a005645.

[15]. Kononenko NL, Haucke V, Molecular mechanisms of presynaptic membrane retrieval and synaptic vesicle reformation, Neuron, 85 (2015) 484–496. [PubMed: 25654254]

[16]. Gan Q, Watanabe S, Synaptic Vesicle Endocytosis in Different Model Systems, Front Cell Neurosci, 12 (2018) 171. [PubMed: 30002619]

[17]. Antonny B, Burd C, De Camilli P, Chen E, Daumke O, Faelber K, Ford M, Frolov VA, Frost A, Hinshaw JE, Kirchhausen T, Kozlov MM, Lenz M, Low HH, McMahon H, Merrifield C, Pollard TD, Robinson PJ, Roux A, Schmid S, Membrane fission by dynamin: what we know and what we need to know, EMBO J, 35 (2016) 2270–2284. [PubMed: 27670760]

[18]. Koenig JH, Ikeda K, Disappearance and reformation of synaptic vesicle membrane upon transmitter release observed under reversible blockage of membrane retrieval, J. Neurosci, 9 (1989) 3844–3860. [PubMed: 2573698]

[19]. Takei K, Mundigl O, Daniell L, De Camilli P, The synaptic vesicle cycle: a single vesicle budding step involving clathrin and dynamin, J. Cell Biol, 133 (1996) 1237–1250. [PubMed: 8682861]

[20]. Yamashita T, Hige T, Takahashi T, Vesicle endocytosis requires dynamin-dependent GTP hydrolysis at a fast CNS synapse, Science, 307 (2005) 124–127. [PubMed: 15637282]

[21]. Xu J, McNeil B, Wu W, Nees D, Bai L, Wu LG, GTP-independent rapid and slow endocytosis at a central synapse, Nat. Neurosci, 11 (2008) 45–53. [PubMed: 18066059]

[22]. Park RJ, Shen H, Liu L, Liu X, Ferguson SM, De Camilli P, Dynamin triple knockout cells reveal off target effects of commonly used dynamin inhibitors, J. Cell Sci, 126 (2013) 5305–5312. [PubMed: 24046449]

[23]. Heuser JE, Proceedings: A possible origin of the 'giant' spontaneous potentials that occur after prolonged transmitter release at frog neuromuscular junctions, J Physiol, 239 (1974) 106P–108P.

[24]. Wu XS, Xue L, Mohan R, Paradiso K, Gillis KD, Wu LG, The origin of quantal size variation: vesicular glutamate concentration plays a significant role, J Neurosci, 27 (2007) 3046–3056. [PubMed: 17360928]

[25]. Zhang B, Koh YH, Beckstead RB, Budnik V, Ganetzky B, Bellen HJ, Synaptic vesicle size and number are regulated by a clathrin adaptor protein required for endocytosis, Neuron, 21 (1998) 1465–1475. [PubMed: 9883738]

[26]. Lisman JE, Raghavachari S, Tsien RW, The sequence of events that underlie quantal transmission at central glutamatergic synapses, Nat. Rev. Neurosci, 8 (2007) 597–609. [PubMed: 17637801]

[27]. He L, Xue L, Xu J, McNeil BD, Bai L, Melicoff E, Adachi R, Wu LG, Compound vesicle fusion increases quantal size and potentiates synaptic transmission, Nature, 459 (2009) 93–97. [PubMed: 19279571]

[28]. Heerssen H, Fetter RD, Davis GW, Clathrin dependence of synaptic-vesicle formation at the Drosophila neuromuscular junction, Curr. Biol, 18 (2008) 401–409. [PubMed: 18356056]

[29]. Kasprowicz J, Kuenen S, Miskiewicz K, Habets RL, Smitz L, Verstreken P, Inactivation of clathrin heavy chain inhibits synaptic recycling but allows bulk membrane uptake, J. Cell Biol, 182 (2008) 1007–1016. [PubMed: 18762582]

[30]. Sato K, Ernstrom GG, Watanabe S, Weimer RM, Chen CH, Sato M, Siddiqui A, Jorgensen EM, Grant BD, Differential requirements for clathrin in receptor-mediated endocytosis and maintenance of synaptic vesicle pools, Proc. Natl. Acad. Sci. U. S. A, 106 (2009) 1139–1144. [PubMed: 19151157]

[31]. Watanabe S, Trimbuch T, Camacho-Perez M, Rost BR, Brokowski B, Sohl-Kielczynski B, Felies A, Davis MW, Rosenmund C, Jorgensen EM, Clathrin regenerates synaptic vesicles from endosomes, Nature, 515 (2014) 228–233. [PubMed: 25296249]

[32]. Kononenko NL, Puchkov D, Classen GA, Walter AM, Pechstein A, Sawade L, Kaempf N, Trimbuch T, Lorenz D, Rosenmund C, Maritzen T, Haucke V, Clathrin/AP-2 Mediate Synaptic Vesicle Reformation from Endosome-like Vacuoles but Are Not Essential for Membrane Retrieval at Central Synapses, Neuron, 82 (2014) 981–988. [PubMed: 24908483]

[33]. Granseth B, Odermatt B, Royle SJ, Lagnado L, Clathrin-mediated endocytosis is the dominant mechanism of vesicle retrieval at hippocampal synapses, Neuron, 51 (2006) 773–786. [PubMed: 16982422]

[34]. Ferguson SM, Brasnjo G, Hayashi M, Wolfel M, Collesi C, Giovedi S, Raimondi A, Gong LW, Ariel P, Paradise S, O'toole E, Flavell R, Cremona O, Miesenbock G, Ryan TA, De Camilli P, A selective activity-dependent requirement for dynamin 1 in synaptic vesicle endocytosis, Science, 316 (2007) 570–574. [PubMed: 17463283]

[35]. Raimondi A, Ferguson SM, Lou X, Armbruster M, Paradise S, Giovedi S, Messa M, Kono N, Takasaki J, Cappello V, O'toole E, Ryan TA, De Camilli P, Overlapping role of dynamin isoforms in synaptic vesicle endocytosis, Neuron, 70 (2011) 1100–1114. [PubMed: 21689597]

[36]. Sankaranarayanan S, Ryan TA, Calcium accelerates endocytosis of vSNAREs at hippocampal synapses, Nat. Neurosci, 4 (2001) 129–136. [PubMed: 11175872]

[37]. Sun T, Wu XS, Xu J, McNeil BD, Pang ZP, Yang W, Bai L, Qadri S, Molkentin JD, Yue DT, Wu LG, The role of calcium/calmodulin-activated calcineurin in rapid and slow endocytosis at central synapses, J Neurosci, 30 (2010) 11838–11847. [PubMed: 20810903]

[38]. Kavalali ET, Jorgensen EM, Visualizing presynaptic function, Nat. Neurosci, 17 (2014) 10–16. [PubMed: 24369372]

[39]. Wu XS, Lee SH, Sheng J, Zhang Z, Zhao WD, Wang D, Jin Y, Charnay P, Ervasti JM, Wu LG, Actin Is Crucial for All Kinetically Distinguishable Forms of Endocytosis at Synapses, Neuron, 92 (2016) 1020–1035. [PubMed: 27840001]

[40]. Wu XS, McNeil BD, Xu J, Fan J, Xue L, Melicoff E, Adachi R, Bai L, Wu LG, Ca(2+) and calmodulin initiate all forms of endocytosis during depolarization at a nerve terminal, Nat. Neurosci, 12 (2009) 1003–1010. [PubMed: 19633667]

[41]. Hosoi N, Holt M, Sakaba T, Calcium dependence of exo- and endocytotic coupling at a glutamatergic synapse, Neuron, 63 (2009) 216–229. [PubMed: 19640480]

[42]. Jin YH, Wu XS, Shi B, Zhang Z, Guo XL, Gan L, Chen ZQ, Wu LG, Protein Kinase C and Calmodulin Serve As Calcium Sensors for Calcium-Stimulated Endocytosis at Synapses, Journal of Neuroscience, 39 (2019) 9478–9490. [PubMed: 31628181]

[43]. Wu XS, Subramanian S, Zhang Y, Shi B, Xia J, Li T, Guo X, El-Hassar L, Szigeti-Buck K, Henao-Mejia J, Flavell RA, Horvath TL, Jonas EA, Kaczmarek LK, Wu LG, Presynaptic Kv3 channels are required for fast and slow endocytosis of synaptic vesicles, Neuron, 109 (2021) 938–946 e935. [PubMed: 33508244]

[44]. Wu Y, O'Toole ET, Girard M, Ritter B, Messa M, Liu X, McPherson PS, Ferguson SM, De Camilli P, A dynamin 1-, dynamin 3- and clathrin-independent pathway of synaptic vesicle recycling mediated by bulk endocytosis, Elife, 3 (2014) e01621. [PubMed: 24963135]

[45]. Matthews G, Sterling P, Evidence that vesicles undergo compound fusion on the synaptic ribbon, J. Neurosci, 28 (2008) 5403–5411. [PubMed: 18495874]

[46]. Ge L, Shin W, Wu L-G, Visualizing sequential compound fusion and kiss-and-run in live excitable cells, bioRxiv, (2021) 2021.2006.2021.449230.

[47]. Chiang HC, Shin W, Zhao WD, Hamid E, Sheng J, Baydyuk M, Wen PJ, Jin A, Momboisse F, Wu LG, Post-fusion structural changes and their roles in exocytosis and endocytosis of dense-core vesicles, Nat. Commun, 5 (2014) 3356. [PubMed: 24561832]

[48]. Lou X, Paradise S, Ferguson SM, De Camilli P, Selective saturation of slow endocytosis at a giant glutamatergic central synapse lacking dynamin 1, Proc. Natl. Acad. Sci. U. S. A, 105 (2008) 17555–17560. [PubMed: 18987309]

[49]. Mettlen M, Chen PH, Srinivasan S, Danuser G, Schmid SL, Regulation of Clathrin-Mediated Endocytosis, Annu. Rev. Biochem, 87 (2018) 871–896. [PubMed: 29661000]

[50]. Fox GQ, Kriebel ME, Dynamic responses of presynaptic terminal membrane pools following KCl and sucrose stimulation, Brain Res, 755 (1997) 47–62. [PubMed: 9163540]

[51]. Sankaranarayanan S, Ryan TA, Real-time measurements of vesicle-SNARE recycling in synapses of the central nervous system, Nat. Cell Biol, 2 (2000) 197–204. [PubMed: 10783237]

[52]. Zhu Y, Xu J, Heinemann SF, Two pathways of synaptic vesicle retrieval revealed by single-vesicle imaging, Neuron, 61 (2009) 397–411. [PubMed: 19217377]

[53]. Zhang Z, Wang D, Sun T, Xu J, Chiang HC, Shin W, Wu LG, The SNARE proteins SNAP25 and synaptobrevin are involved in endocytosis at hippocampal synapses, J. Neurosci, 33 (2013) 9169–9175. [PubMed: 23699527]

[54]. Wu XS, Zhang Z, Zhao WD, Wang D, Luo F, Wu LG, Calcineurin is universally involved in vesicle endocytosis at neuronal and nonneuronal secretory cells, Cell Rep, 7 (2014) 982–988. [PubMed: 24835995]

Highlights

- Dynamin 1 controls vesicle size by regulating membrane pit size
- Dynamin 1 is more crucial for endocytosis than recognized at synapses

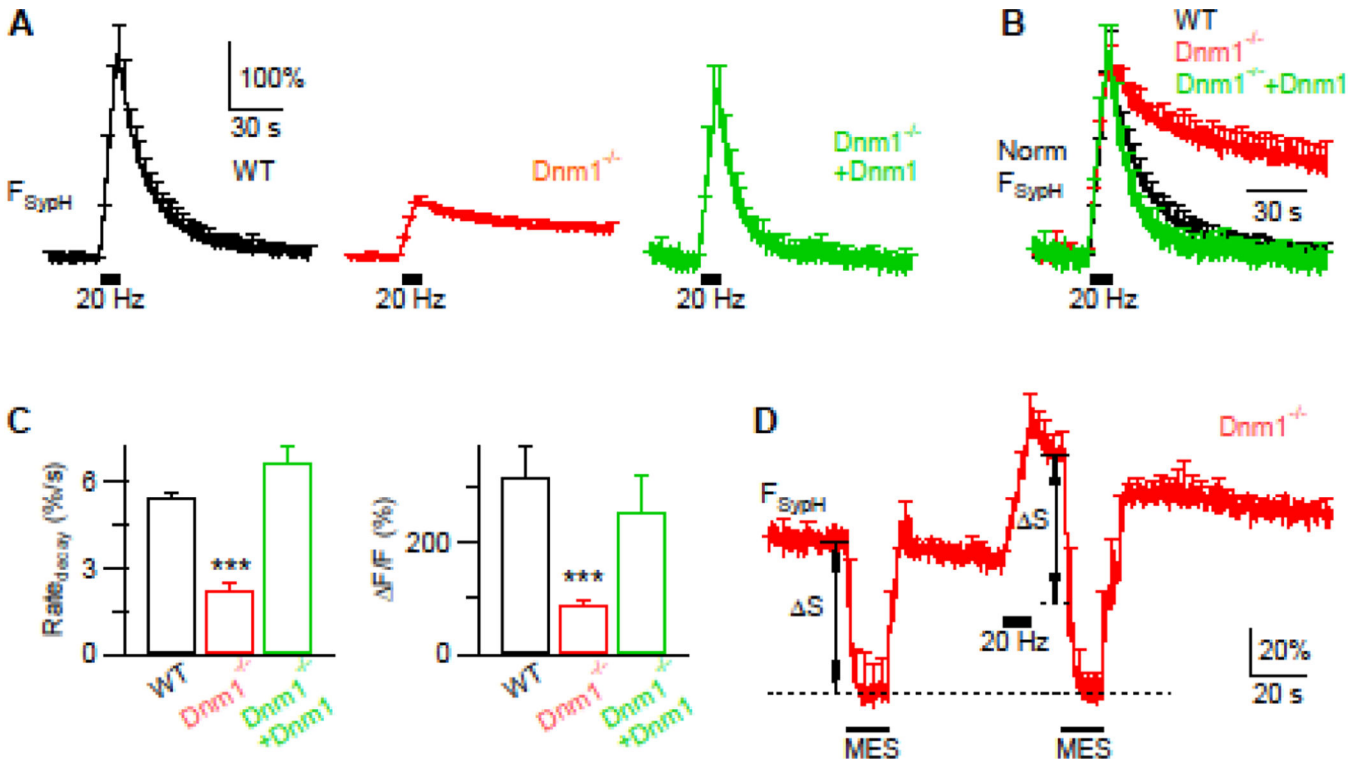

Figure 1.

Dynamin 1 knockout severely inhibits endocytosis after repetitive firing at 20 Hz at hippocampal synapses. **A-C,** F_{SypH} traces (A, B), $Rate_{decay}$ (C, left) and ΔF/F (C, right) induced by $Train_{20Hz}$ (10 s train of action potentials at 20 Hz) in wild-type (WT) cultures (n = 10 experiments), $Dnm1^{-/-}$ cultures (n = 6 experiments), and $Dnm1^{-/-}$ hippocampal cultures overexpressed with WT dynamin 1 ($Dnm1^{-/-}$ + Dnm1; containing mCherry for recognition, n = 5). F_{SypH} traces in panel B are the same as those in panel A, but with the peak F_{SypH} rescaled (Norm F_{SypH}) to the same amplitude for better comparison of their time courses. Temperature (applies to Figs. 1–4): 22–24°C. Data expressed as mean+s.e.m (applies to Figs 1–4). ***: $p < 0.001$ (t test, compared to WT).

D, Applying MES solution (pH: 5.5) quenched F_{SypH} (mean + s.e.m.) to a similar level (lowest dash line) before and after a 10 s train of stimuli in $Dnm1^{-/-}$ cultures (n = 5 experiments, 22–24°C). Δ*S*: SypH at resting plasma membrane quenched by MES (see main text for more description).

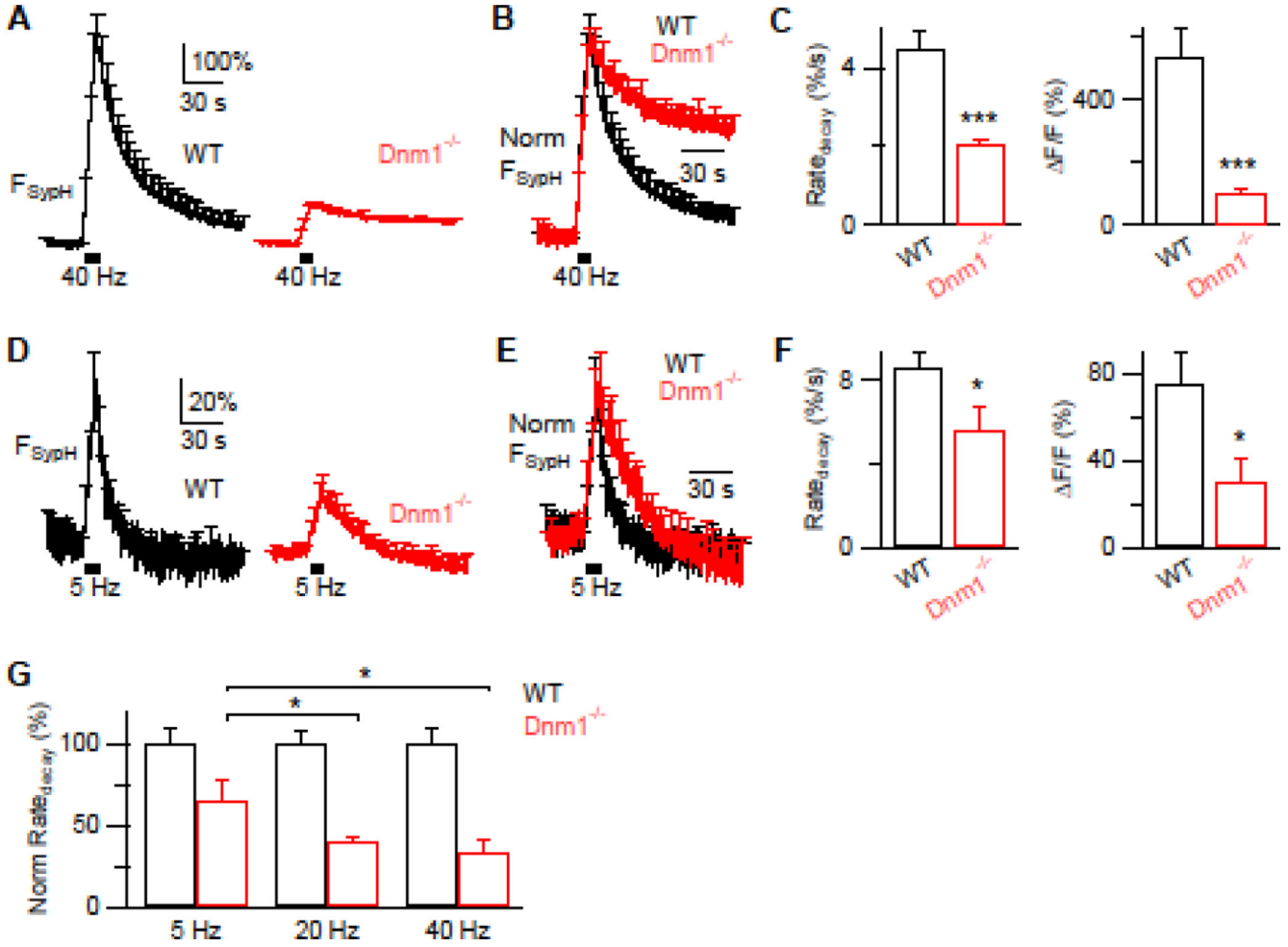

Figure 2.

Dynamin 1 knockout inhibits endocytosis after repetitive firing at 5 and 40 Hz at hippocampal synapses. **A-C,** F_{SypH} traces (A, B), $Rate_{decay}$ (C, left) and ΔF/F (C, right) induced by a 10-s train of action potentials at 40 Hz) in wild-type (WT) cultures (n = 14 experiments) and Dnm1$^{-/-}$ cultures (n = 6 experiments). F_{SypH} traces in panel B are the same as those in panel A, but with the peak F_{SypH} rescaled to the same amplitude for better comparison of time courses. Data expressed as mean + s.e.m.; ***: $p < 0.001$ (t test, compared to WT).

D-F, Similar arrangement as A-C respectively, except that the stimulation was a 10 s train of action potentials at 5 Hz (WT, 9 experiments; Dnm1$^{-/-}$, 8 experiments), *: $p < 0.05$ (t test, compared to WT).

G, $Rate_{decay}$ after 5, 20, and 40 Hz action potential train in the WT and Dnm1$^{-/-}$ cultures. For each frequency of stimulation, $Rate_{decay}$ was normalized to the mean of the corresponding WT $Rate_{decay}$. This plot aims to compare the degree of reduction of $Rate_{decay}$ at different frequencies. 5 Hz: WT, n = 9; Dnm1$^{-/-}$, n = 8 (original data from Fig. 2D–F). 20 Hz: WT, n = 10, Dnm1$^{-/-}$, n = 6 (original data from Fig. 1A–C). 40 Hz: WT, n = 14, Dnm1$^{-/-}$, n = 5 (original data from Fig. 2A–C). *: $p < 0.05$ (t test); ***: $p < 0.001$.

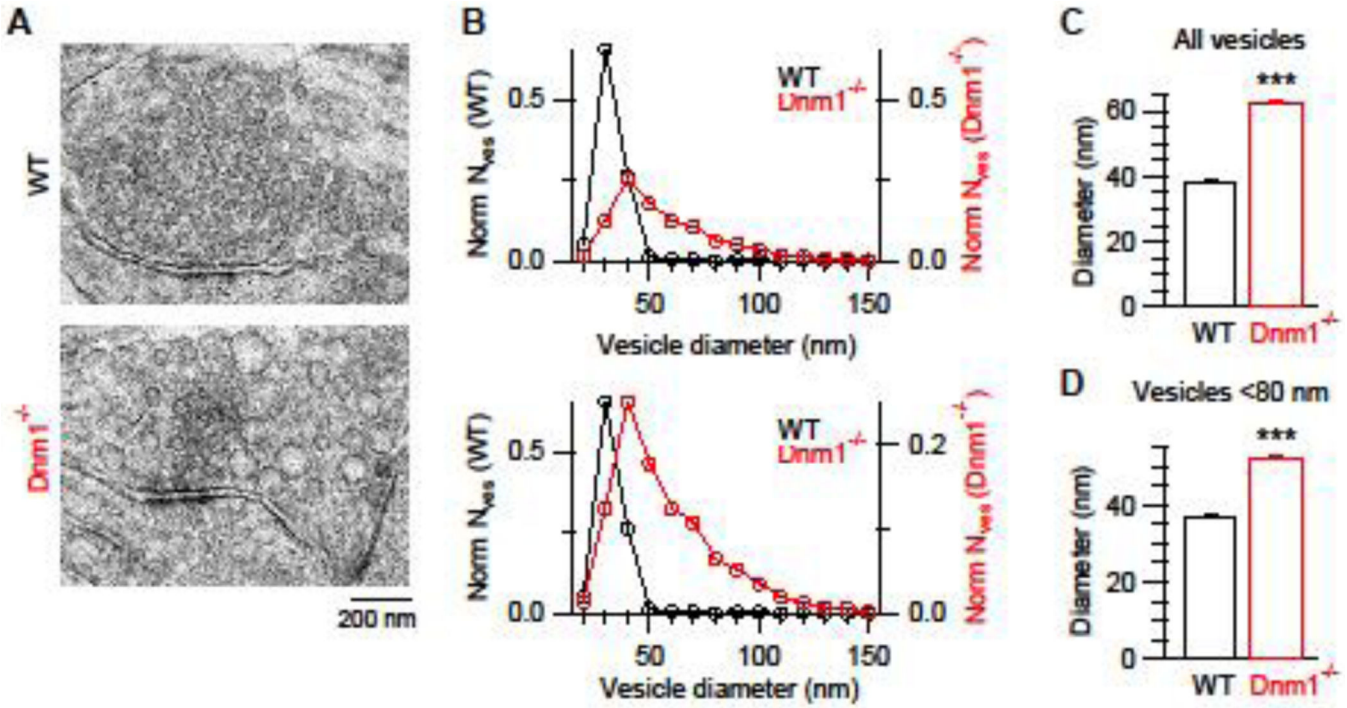

Figure 3.

Dynamin 1 knockout significantly increases vesicle size at hippocampal synapses. **A,** Electron microscopic image of synaptic boutons from wild-type (WT) or Dnm1$^{-/-}$ hippocampal culture.

B, Upper: Vesicle diameter distribution: The normalized number of vesicles (Norm N_{ves}) plotted versus the vesicle diameter in WT (left axis) and Dnm1$^{-/-}$ (right axis) hippocampal cultures. Vesicles with a diameter difference within 10 nm are binned together. The total vesicle number is normalized as 1 for each group of data. WT: 2170 vesicles, 22 boutons, 4 cultures, each culture from 6 mice; Dnm1$^{-/-}$: 2628 vesicles, 49 boutons, 5 cultures, each culture from 3–5 mice.

Lower: Same as in left panel, but with the WT and Dnm1$^{-/-}$ data plotted at different scales such that the peak N_{ves} (norm) for WT and Dnm1$^{-/-}$ cultures is at the same vertical level. A clear right shift of the distribution was observed for Dnm1$^{-/-}$ cultures.

C, Mean (+ s.e.m.) vesicle diameter from WT (2170 vesicles) and Dnm1$^{-/-}$ (2628 vesicles) cultures. ***: $p < 0.001$, t test. Vesicles with a diameter between 20–315 nm are all included.

D, Mean (+ s.e.m.) vesicle diameter for vesicles with a diameter less than 80 nm from WT (2101 vesicles) and Dnm1$^{-/-}$ (2146 vesicles) cultures. *** $p < 0.001$ (t test).

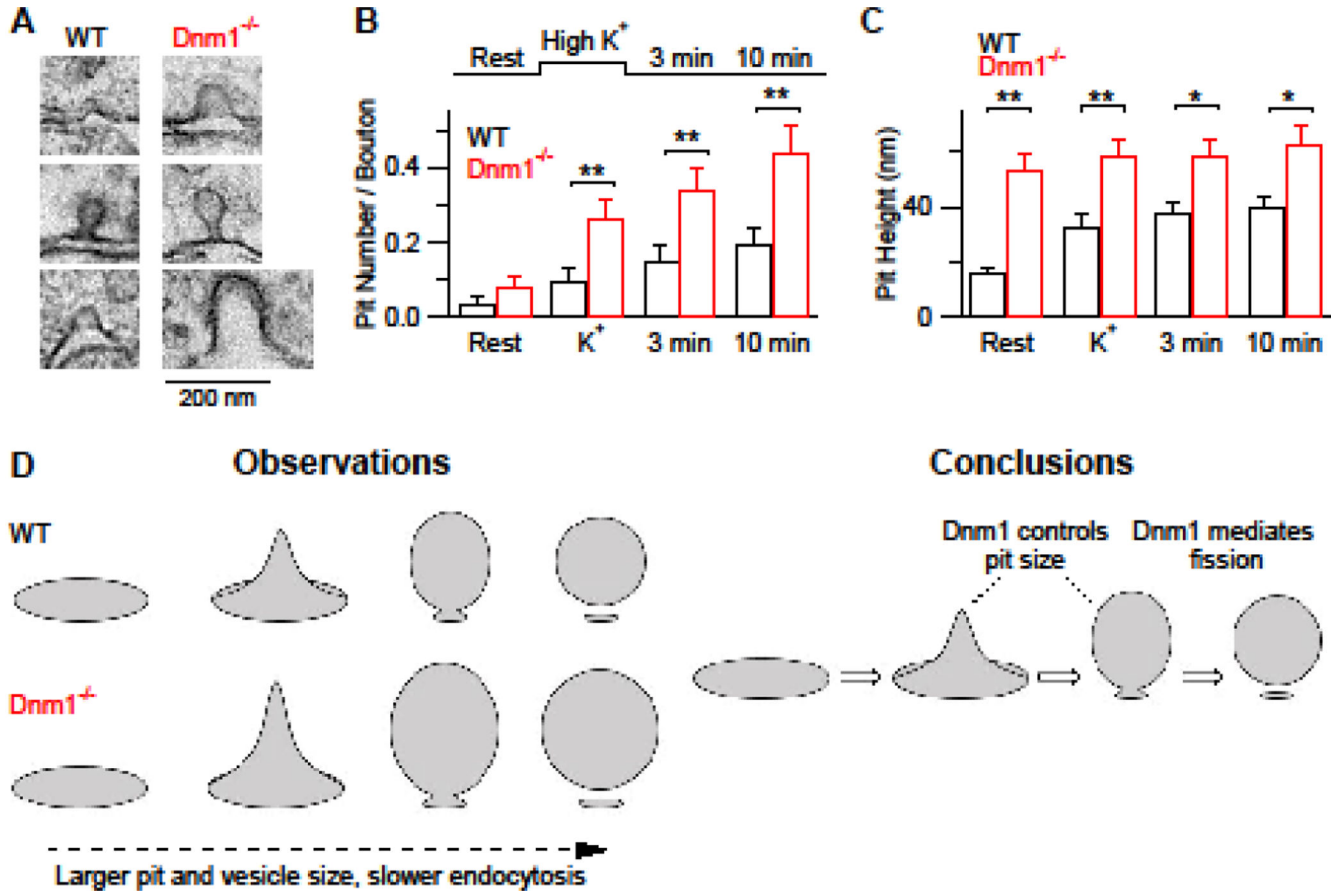

Figure 4.

Dynamin 1 knockout significantly increases membrane pit size at hippocampal synapses. **A,** Sampled EM images of membrane pits from WT (left) and Dnm1$^{-/-}$ (right) boutons. **B-C,** The number of pits per bouton cross section (B) and the pit height (C) before (Rest) and at 0, 3, and 10 min after KCl application (90 mM, 1.5 min) in WT and Dnm1$^{-/-}$ boutons. Data at each time point (each bar) were from 110 bouton cross sections, 3 cultures; and each culture was from 3–5 mice. **D,** A schematic summary of our main observations and conclusions. Observations (left): Dnm1 KO increases pit size and slows endocytosis. Conclusions: Dnm1 controls pit size and mediates fission.